

# Novel Fluorescein-Based Fluorophores: Synthesis, Photophysics and Micro-Environmental Study

Rahul Telore<sup>1</sup> · Santosh Chemate<sup>1</sup> · Vikas Padalkar<sup>1</sup> · Nagaiyan Sekar<sup>1</sup>

Received: 22 May 2015 / Accepted: 28 September 2015 / Published online: 13 October 2015  
© Springer Science+Business Media New York 2015

**Abstract** Carboxylic acid substituted fluorescein derivatives were synthesized from 2,4-dihydroxy carboxylic acid and phthalic anhydride or trimellitic anhydride. The photophysical properties like absorption, emission and fluorescence quantum yields of these fluorophores were studied. The conjugation studies of these fluorophores with different proteins at different concentrations were carried out. The effect of pH on photophysical properties was studied at different pH ranges from 5 to 12. The change in the absorption and emission with respect to viscosity of medium was also studied. The changes in the electronic transition, energy levels, and orbital diagram of the fluorescein derivatives were computed using the TD-DFT computations and co-related with experimental photophysical data.

**Keywords** Fluorescein · Photophysics · TD-DFT · pH · Proteins · Conjugation

---

**Electronic supplementary material** The online version of this article (doi:10.1007/s10895-015-1676-0) contains supplementary material, which is available to authorized users.

---

✉ Nagaiyan Sekar  
n.sekar@ictmumbai.edu.in

<sup>1</sup> Dyestuff Technology Department, N. P. Marg, Tinctorial Chemistry Group, Institute of Chemical Technology Matunga, Mumbai 400 019, India

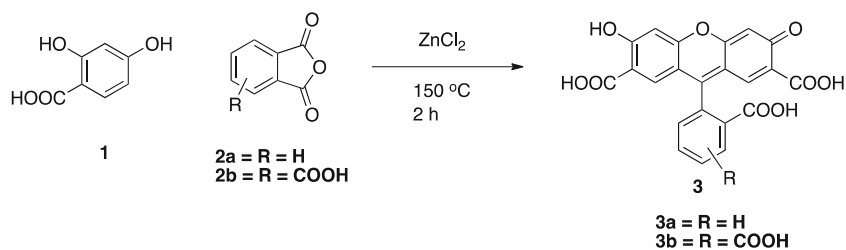
## Introduction

Organic fluorophores are of great interest in a wide variety of applications [1–3]. They act as promising candidates for developing electronic and biological devices [4–7]. Molecules with efficient fluorescence include aromatic hydrocarbons and their derivatives [8]. The commonly used fluorophores are planar  $\pi$ -conjugated organic dyes and linearly bonded fluorophores which includes xanthenes [9], perylenes [10], boron-dipyrromethene [11], squaraine [12] and cyanine dyes [13]. The planar conjugated molecules show high fluorescence quantum efficiencies and high molar extinction coefficient over linearly conjugated fluorophores but poor solubility in polar as well as non-polar solvents [6].

Rhodamine and fluorescein derivatives are important planar  $\pi$ -conjugated water soluble fluorophores [6]. The quantum efficiencies and photostabilities of these fluorophores are more as compared to other water soluble fluorophores [6]. The production cost of these dyes is very less and they are commercially used in various high-tech applications such as fluorescent probes [4], metal sensors [14], pH sensors [15], explosive detectors [16–18], lasers [19] and in dye-sensitized solar cells [20, 21]. The xanthene derivatives contain free carboxylic acid functional groups available for conjugation with different biomolecules in biosensing applications [22–25].

Therefore, large  $\pi$ -conjugated xanthene derivatives possessing high solubility in various solvents and desirable optical characteristics are continually required and their development has led to the rapid proliferation of advanced fluorescence-based techniques, the biggest growth areas being biology, medicine, chemistry, and material science.

In present paper, we have synthesized novel fluorescent probes based on fluorescein core owing to their excellent photophysical properties such as high molar extinction coefficient, high fluorescence quantum yield, excitation and

**Scheme 1** Synthesis of 3a and 3b

emission at longer wavelength [26, 27]. Fluorescein-5-isothiocyanate (FITC) is used in microscopy studies of biological samples and as fluorescent probes in immunoassays [28]. FITC shows strong single absorption at 492 nm with high molar extinction coefficient ( $80,000 \text{ M}^{-1} \text{ cm}^{-1}$ ) and emit at 512 nm with good absolute quantum yield (0.90) [29] whereas fluorescence quenching is noted after binding with proteins [30].

Depending upon pH, fluorescein can exist in four different prototropic forms (monoanion, dianion, neutral, and cation), which have significantly different absorption/emission properties. The steep pH dependence is a considerable drawback of fluorescein in biological study.

## Experimental

### Reagents and Analysis Methods

#### Methods and Instruments

All the synthesized compounds were purified by crystallisation followed by column chromatography on silica gel. The compounds 3a and 3b were characterized by  $^1\text{H}$ -NMR,  $^{13}\text{C}$ -NMR, and mass techniques. The  $^1\text{H}$ -NMR spectra were recorded on a Varian (500 MHz) spectrometer and  $^{13}\text{C}$ -NMR spectra on a Varian (125 MHz) spectrometer, and all spectra were recorded in a  $\text{D}_2\text{O}$  and  $\text{DMSO}-d_6$  solvent using TMS as an internal reference standard at room

temperature ( $20^\circ\text{C}$ ). Chemical shifts of NMR spectra are given in parts per million (ppm). The FT-IR spectra were recorded on a Jasco 4100 Fourier Transform IR instrument (ATR accessories). Mass spectra were recorded on Jeol mass spectrometer of AccuTOF GCV model and EI source with mass resolution 6000.

#### UV Absorption Spectra

Absorption spectra were recorded on a Perkin-Elmer Lambda-25 spectrophotometer in 1 cm length quartz cell. All the samples were measured from  $1 \times 10^{-6} \text{ mol L}^{-1}$  solution with the wavelength range between 200 and 800 nm at room temperature ( $25^\circ\text{C}$ ).

#### Fluorescence Emission Spectra

Fluorescence emission spectra were measured on Varian Cary Eclipse fluorescence spectrophotometer with slit width of 2.5 nm. The source of light used for fluorescence measurement was Xenon flash lamp. The emission spectra were obtained from  $1 \times 10^{-6} \text{ mol L}^{-1}$  solution at room temperature ( $25^\circ\text{C}$ ). The excitation wavelength was absorption maxima of the corresponding compound.

#### Quantum Yield

The quantum yields of the compounds were evaluated in solvent. The comparative method was used for quantum yield

**Table 1** Observed and computed absorption and emission of compounds 3a and 3b

Comps.	$\lambda_{\text{abs}}^a$ (nm)	$\epsilon^b$ ( $\text{dm}^3 \text{ mol}^{-1} \text{ cm}^{-1}$ )	Vertical Excitation		$f^c$	%D <sup>d</sup>	Assignment <sup>e</sup>	$\lambda_{\text{emi}}^f$ (nm)	Stoke's Shift (nm)	TD-DFT emission (nm)	%D <sup>d</sup>	%Φ <sup>g</sup>
			nm	eV								
3a	490	16086	427	2.902	0.425	12	H→L (89 %)	511	21	496	2.9	56
3b	492	19812	427	2.898	0.420	12	H→L (89 %)	515	23	495	3.8	59

<sup>a</sup> Absorption wavelengths were measured in water at room temperature

<sup>b</sup> Molar extinction coefficient

<sup>c</sup> Oscillator Strength

<sup>d</sup> % deviation between experimental absorption/emission and computed absorption/emission

<sup>e</sup> Orbital contribution, H: HOMO; L: LUMO

<sup>f</sup> Emission wavelengths were measured in water at room temperature

<sup>g</sup> Φ: Quantum yields

**Table 2** Absorption maxima ( $\lambda_{\text{abs}}$ , nm), Full width half maxima (FWHM) (nm), molar extinction coefficient ( $\epsilon$   $\text{M}^{-1}\text{cm}^{-1}$ ), integrated absorption coefficient (IAC), oscillator strength ( $f$ ) and transition dipole moment (D) of compound 3a and 3b

Compd.	$\lambda_{\text{max}}$ (nm)	FWHM (nm)	$\epsilon$ ( $\text{Mole}^{-1}\text{cm}^{-1}$ )	IAC	$f$	TDM (D)
3a	490	32	16,086	6,233,685.14	0.027	1.68
3b	492	34	19,812	7,743,096.12	0.033	1.86

determination [31]. Fluorescein ( $\phi$ : 0.92 in 0.1 N NaOH) was used as standard [32]. All the measurements were performed at room temperature (25 °C).

#### pH and Viscosity Study

The pH study was carried out by using phosphate buffer (20 mM) solution of pH range 5–12. Millipore water was used for preparation of buffer solution. The effect of viscosity on absorption and emission were carried out at different viscosities. The glycerol was used for viscosity adjustment. All absorption and emission measurements were carried out at room temperature (25 °C) and concentration of solution was  $1 \times 10^{-6}$  mol.  $\text{L}^{-1}$ .

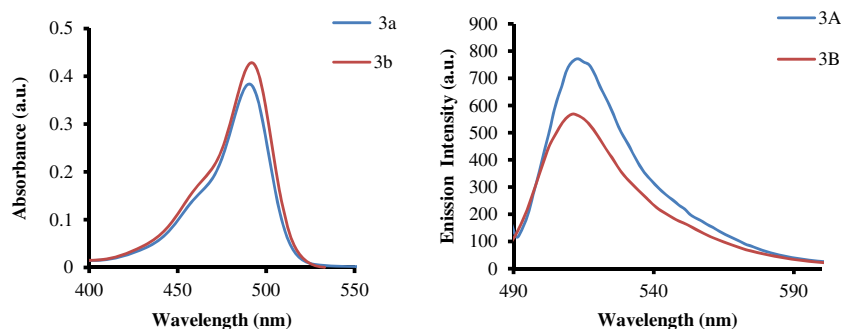
#### Conjugation Study

Bovine serum albumin (BSA), Egg Albumin and Gelatin were used for conjugation study. The conjugations were performed using carbodiimide chemistry as per reported procedure [22, 33]. A different protein: dye molar concentration was used for bioconjugation study. All the bioconjugation experiments were carried out in phosphate buffers (20 mM) of pH 7.4, which was prepared in millipore double distilled water. The stock solution of protein and fluorophores were prepared in pH 7.4 phosphate buffer, and the final reaction volume of the protein-fluorophore conjugates was kept constant at 3 mL for each preparation. The fluorophores were activated by using *N*-(3-dimethylaminopropyl)-*N*-ethylcarbodiimide hydrochloride (EDC) and *N*-hydroxysuccinimide (NHS) for 4 h at room temperature

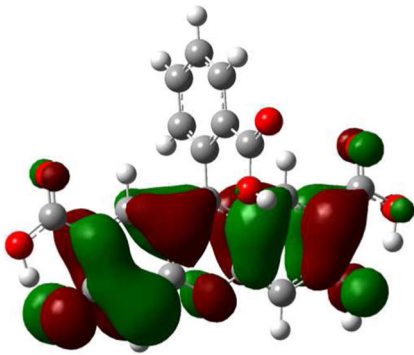
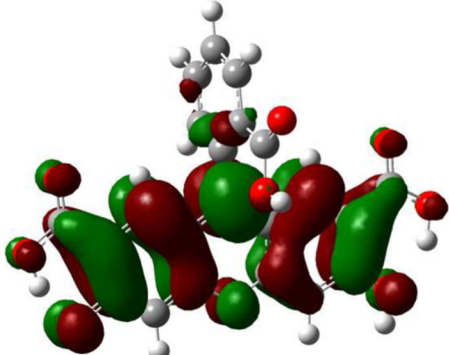
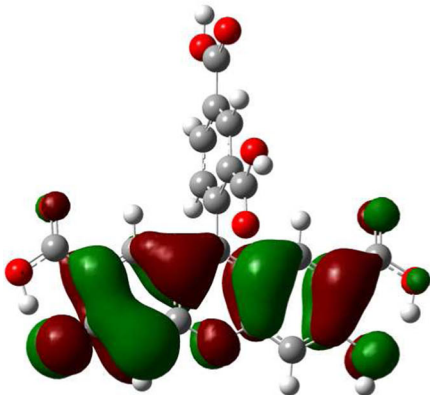
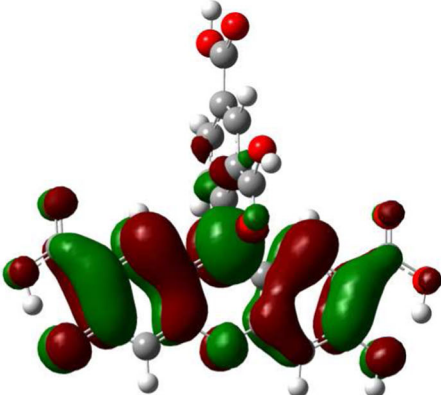
(25 °C) and then centrifuged for 10 min to remove the urea precipitate. The supernatant was used to prepare the conjugates with protein by adding different amounts of fluorophores to a fixed amount of protein (1 mg) in a final volume of 3 mL to make protein-hapten conjugates of different molar ratios. The conjugations were performed for 12 h at room temperature (25 °C). The conjugates were purified by dialysis thrice. The obtained conjugates were used for measurements of absorption and emission properties.

#### Computational Methods

The ground state geometries of the compounds 3a–3b in their  $C_1$  symmetry were optimized using the tight criteria in the gas phase using (DFT) [34]. The functional used in this study was B3LYP [35]. The basis set used for all atoms was 6-31G(d) [35, 36] for all the atoms. The vibrational frequencies of the optimized structures were computed using the same method to verify that the optimized structures correspond to local minima on the potential energy surface. The vertical excitation energies at the ground-state equilibrium geometries were calculated with TD-DFT [37–39]. The low-lying first singlet excited state ( $S_1$ ) of each tautomer was relaxed using TD-DFT to obtain its minimum energy geometry. The difference between the energies of the optimized geometries in the first singlet excited state and the ground state was used in computing the emissions [40]. All electronic structure computations were carried out using Gaussian 09 program [41].

**Fig. 1** Absorption and emission spectra of the fluorophores 3a and 3b

**Table 3** Frontier molecular orbitals of compounds 3a and 3b

Comps.	HOMO	LUMO
3a		
3b		

### Synthesis of Fluorophores

#### General Procedure for Synthesis of Compounds 3a and 3b

The mixture of 2,4-dihydroxybenzoic acid 1 (88 mmol) and anhydrides 2a–2b (44 mmol) was heated at 150 °C for 2 h in presence of ZnCl<sub>2</sub> (180 mmol). The reaction mixture was cooled to room temperature and poured over (20 mL) ice water with constant stirring. The precipitated product was filtered, and washed with cold water (25 mL). The crude product was washed by 10 % NaHCO<sub>3</sub> solution (50 mL) (Scheme 1) and dried at room temperature under vacuum. The crude products were purified by column chromatography on silica gel.

#### Spectral Data of Compound 3a

<sup>1</sup>H-NMR(DMSO-*d*<sub>6</sub>, 500 MHz) δ ppm: 6.53 (4H), 6.66 (2H), 7.24 (1H), 7.68–7.71 (t, 1H), 7.76–7.77 (1H), 7.79–7.94 (1H), 10.09 (s, 2H).

<sup>13</sup>C-NMR(DMSO-*d*<sub>6</sub>, 125 MHz), δ ppm: 83.54, 102.69, 110.69, 110.02, 113.06, 124.49, 125.04, 126.62, 129.51, 130.51, 136.04, 152.30, 152.93, 159.93, 169.16.

<sup>1</sup>H-NMR(D<sub>2</sub>O, 500 MHz), δ ppm: 6.52 (4H), 6.66 (2H), 7.20–7.21 (1H), 7.67–7.70 (t, 1H), 7.76–7.78 (1H), 7.78–7.97 (1H).

FT-IR (KBr, cm<sup>-1</sup>): 2962, 1592, 1465, 1111.

Mass: C<sub>22</sub>H<sub>12</sub>O<sub>9</sub>=420.05, Mass=333.1 [M+1] (–2xCOOH: Recorded mass is with positive mode; decarboxylation occurs during ionisation).

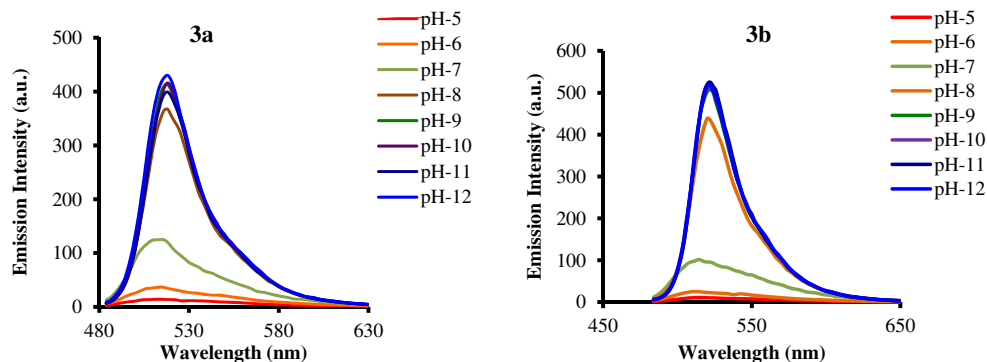
#### Spectral Data of Compound 3b

<sup>1</sup>H-NMR(DMSO-*d*<sub>6</sub>, 500 MHz), δ ppm: 6.68 (s, 1H), 7.37 (d, 1H, *J*=8 Hz), 7.62 (s, 1H), 8.07 (d, 1H, *J*=8.2 Hz), 8.21 (d, 1H, *J*=7.5 Hz), 8.29 (d, 1H, *J*=9.1 Hz), 8.38 (s, 1H), 10.1 (s, 4H).

<sup>13</sup>C-NMR(DMSO-*d*<sub>6</sub>, 125 MHz), δ ppm: 83.85, 102.93, 109.41, 113.3, 124.9, 127.30, 129.86, 131.39, 136.67, 152.35, 153.20, 160.19, 168.54.

FT-IR (KBr, cm<sup>-1</sup>): 2989, 1595, 1471, 1112.

**Fig. 2** Effect of pH on fluorescence emission of the fluorophores 3a and 3b



**Mass:**  $C_{23}H_{12}O_{11}=464.04$ ,  $Mass=377.1$  1 [M+1] ( $-2xCOOH$ : Recorded mass is with positive mode; decarboxylation occurs during ionisation).

## Results and Discussions

The synthesised fluorescein derivatives are structural analogues of FITC dye. The fluorescence quantum efficiencies of the synthesised dyes are lower (3a= $\Phi F$ : 56 % and 3b= $\Phi F$ : 59 %) than FITC ( $\Phi F$ : 90 %). However, synthesised dyes contain more carboxylic acid groups, which increase the water solubility of dyes in water. Taking advantages of water solubility and availability of binding groups the synthesised fluorescein derivatives were further explored for pH, viscosity and bioconjugation study. As the two molecules 3a and 3b contain carboxylic acid and hydroxyl groups, it is expected to get improved water solubility which will facilitate bioconjugation with biomolecules. The resulting fluorescein derivatives were expected to enhance the spectroscopic properties, including fluorescence because slight environmental changes are known to influence fluorescein's emission [34, 35, 37–43]. Viscosity study has showed that fluorescence intensity of the compounds increases with increasing viscosity of the solution (by increasing the amount of glycerol). This may be explained due to restriction of Brownian motion of the molecule's viscous drag. Fluorescence quantum yield in glycerol solution is found greater as compared to non-viscous

solvents. It is well known that, in viscous/rigid medium, most of the fluorescent compounds undergo restriction of intramolecular rotation [44] or restriction of twisted intramolecular charge transfer or restriction of charge transfer process occurs which suppresses the nonradiative pathways and enhances the radiative pathways [44]. In case of 3a and 3b the enhancement of fluorescent intensity in viscous medium can be assigned to above process.

## Synthesis Strategy

The carboxylic acid substituted novel fluorescein derivatives 3a and 3b were prepared by acid catalysed condensation reaction of 2,4-dihydroxy benzoic acid and anhydrides. The fluorophores are purified by acid–base treatments followed by column chromatography on silica gel and characterized by spectral techniques. Carboxylic acid groups are purposefully incorporated in fluorescein core to improve the water solubility of compounds. The compounds 3a and 3b contain three and four carboxylic acid groups respectively. The carboxylic acid groups are further explored for conjugation with proteins using NHS and EDC coupling reaction.

## Photophysical Properties

The dyes 3a and 3b are fluorescent in solution. The absorption and the emission properties of the fluorophores 3a and 3b were evaluated in water because of good solubility of

**Fig. 3** Normalised emission spectra of compounds 3a and 3b at various pH

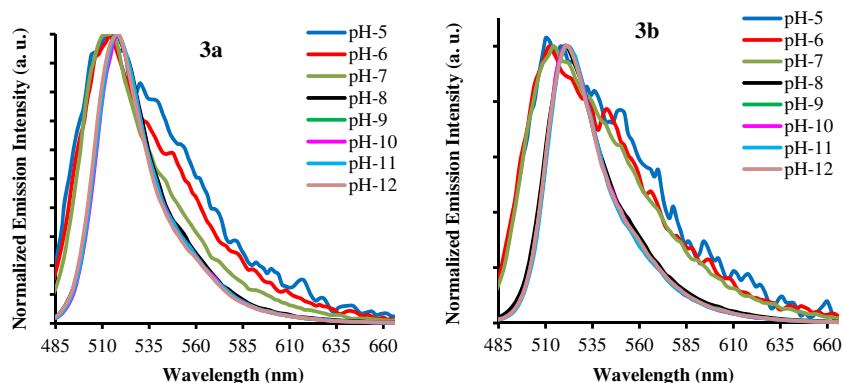
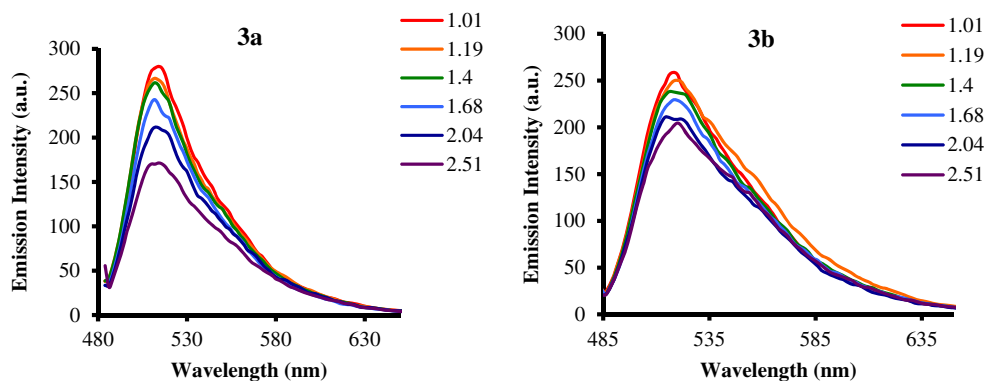


**Fig. 4** Effect of viscosity on fluorescence emission of the fluorophores 3a and 3b



fluorophores in water. The compounds absorb between 490 and 499 nm with high intense emission between 511 and 519 nm. The absorption and emission properties of these compounds are independent of substitution effect. This clearly indicates that xanthene and phthalein moiety is responsible for absorption and emission. The results confirmed that oxidation potential of xanthene moiety and reduction potential of phthalein moiety play an important role in the absorption and emission. The quantum yield of the compounds is around 60 %. It is well known that the quantum efficiencies of the compounds depend on substitution pattern. This hypothesis is no more promising in this particular study. This was understood by correlating study of HOMO energy and quantum yield. Quantum yield of basic moiety of fluorescein di-acid derivative 3a and 3b was calculated to be 56 and 59 % respectively. The frontier molecular orbital diagrams of the compounds 3a and 3b were shown in Table 3.

The photophysical properties of these compounds were evaluated computationally and compared with experimental results. The experimental and theoretical results are in good agreement with each other. The % deviation between experimental absorption and the vertical absorption is 12 % for both the compounds while the % deviation between experimental emission and TD-DFT emission is very less, between

2 and 3.8 %. The absorption, emission, quantum yield and TD-DFT computational data are presented in Tables 1 and 2. The absorption and emission spectra of compounds are presented in Fig. 1. In order to have more understanding of the nature of the electronically excited state, the calculated MOs of 3a and 3b are shown in Table 3. Only the highest occupied molecular orbital and degenerate lowest unoccupied molecular orbitals are shown here. Table 3 illustrates that the HOMO and the LUMO are localized xanthene part for both the molecules. This indicates that charge transfer from xanthene unit to phthalein unit did not occur after photo-excitation. Ground state and excited state geometry of the compounds 3a and 3b were optimized to understand the structural properties of the compounds. The optimized structures are shown in Figure S1 and Figure S2 and structural parameters are summarized in Table S1. In both the compounds phthalein ring is out of plane it's almost perpendicular to xanthene ring. In the case of compound 3a, the ground state and the excited state geometry is almost similar, while in the case of compound 3b, the torsion ( $\theta=105$ ) is more in the excited state in comparison to the ground state ( $\theta=93$ ). This structural property is responsible for restriction charge transfer from xanthene unit to phthaline unit which was supported molecular orbitals.

**Fig. 5** Normalised emission spectra of compounds 3a and 3b at different viscosity

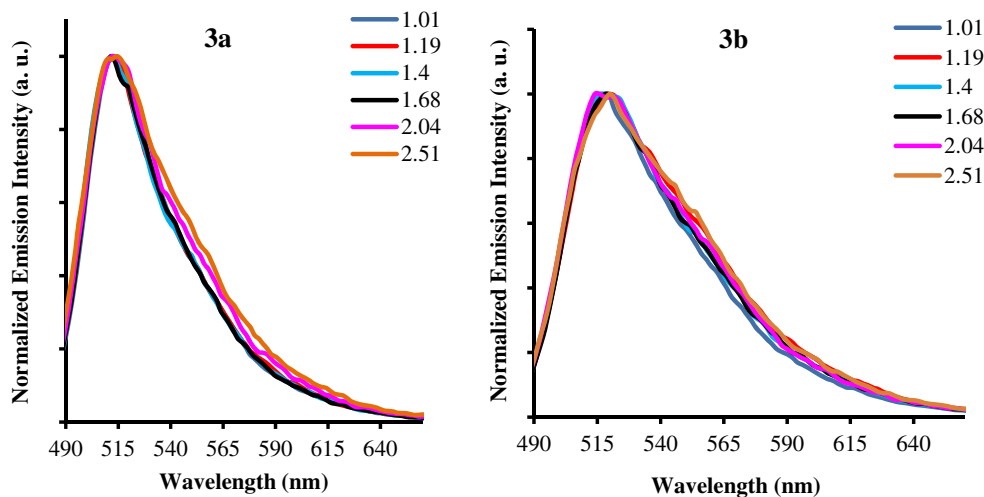
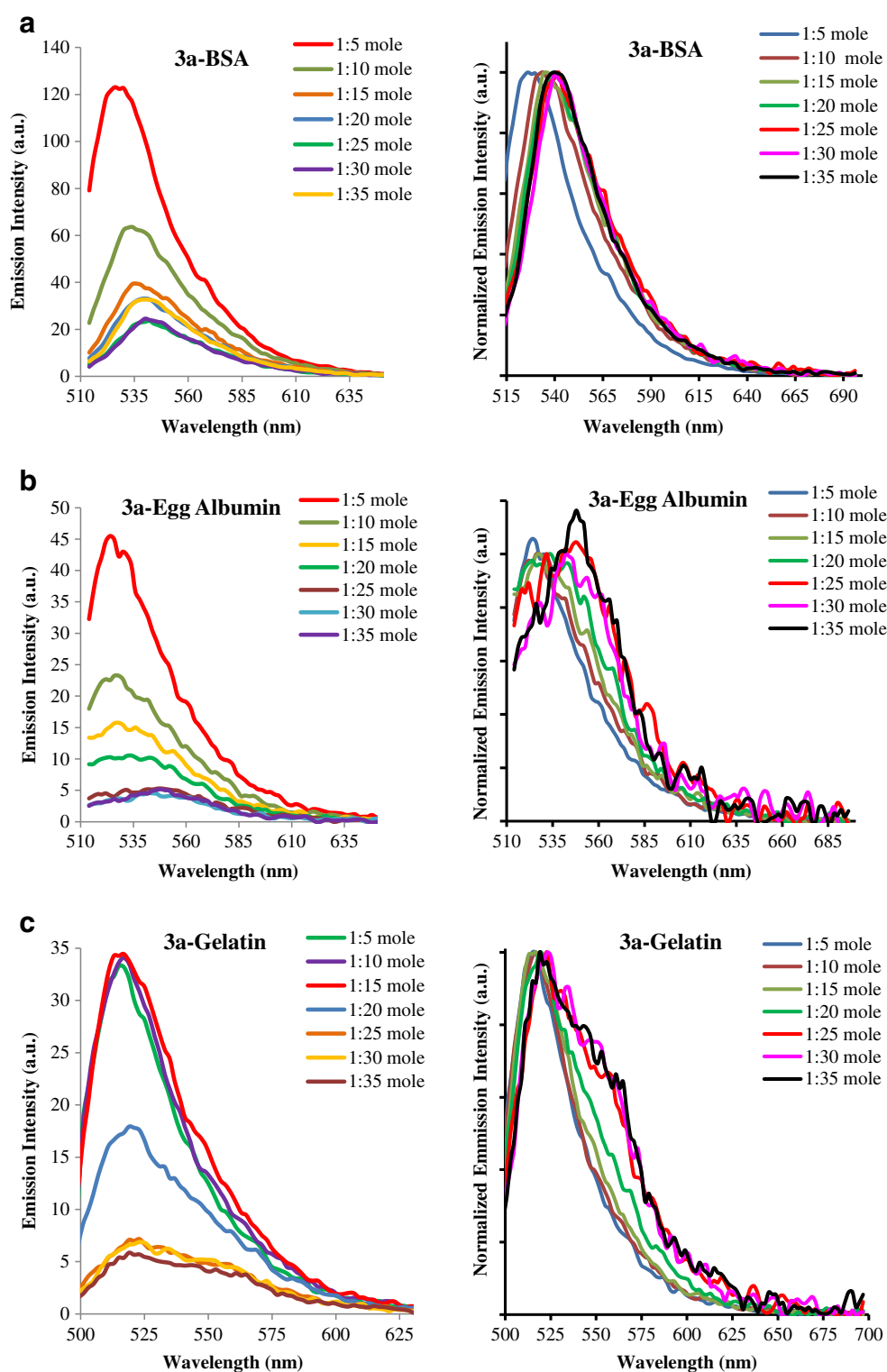


**Fig. 6** **a** Fluorescence spectra of BSA-3a conjugate (*left*) and normalised spectra (*right*). **b** Fluorescence spectra of Egg Albumin-3a conjugate (*left*) and normalised spectra (*right*). **c** Fluorescence spectra of Gelatin-3a conjugate (*left*) and normalised spectra (*right*)

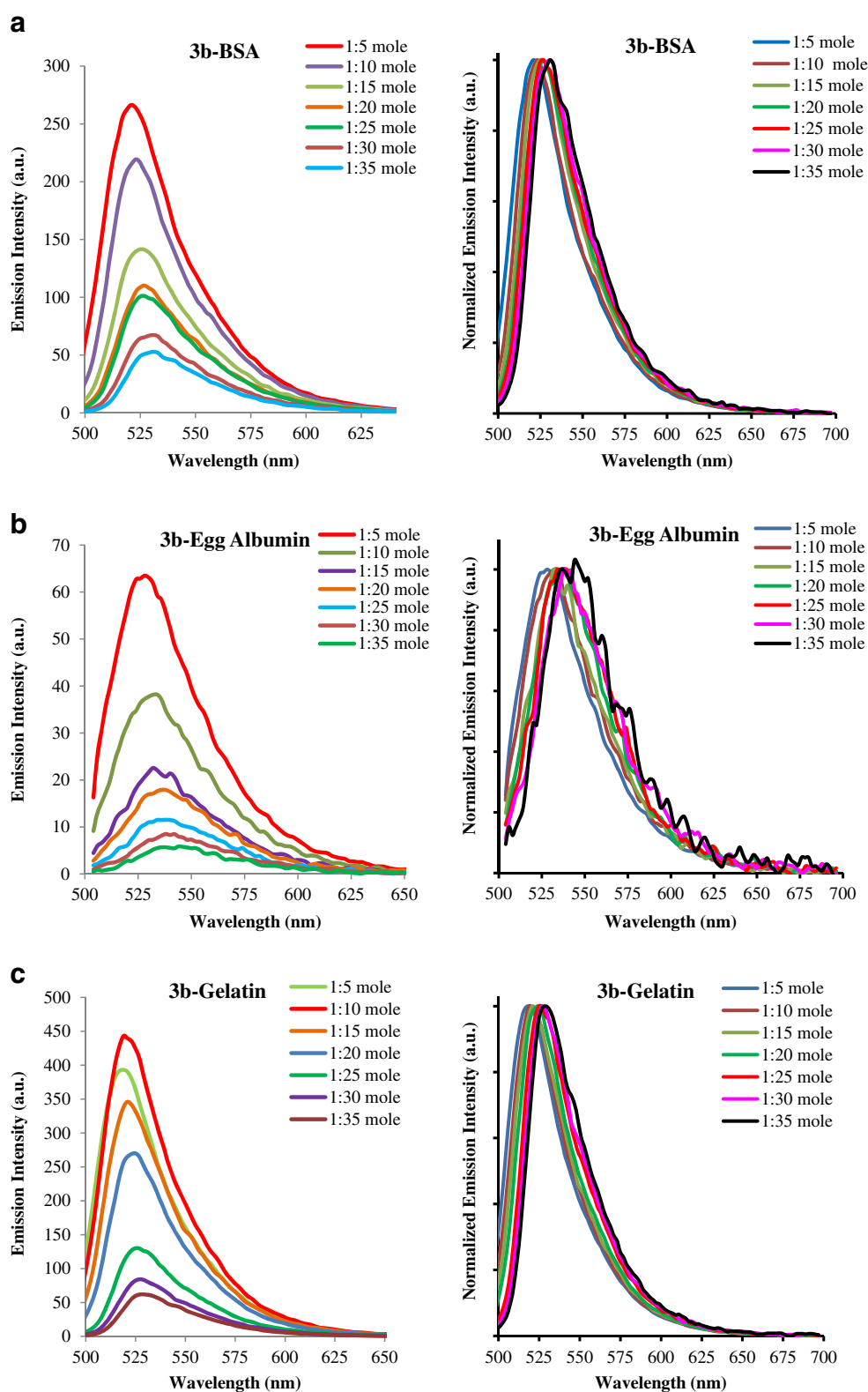


### pH and Viscosity Study

One of the most important requirements of fluorescent dye in biological study is that the fluorophore should have very high fluorescence intensity along with high quantum yield in the biological environment. Along with good fluorescence

properties, the fluorescence emission should be sensitive towards microenvironment like pH, viscosity, hydrogen bonding, and temperature. Here we have studied the effect of pH and viscosity on fluorescence emission of compounds 3a and 3b. The compounds 3a and 3b are sensitive towards pH as well as viscosity. The fluorescence intensity of the synthesized

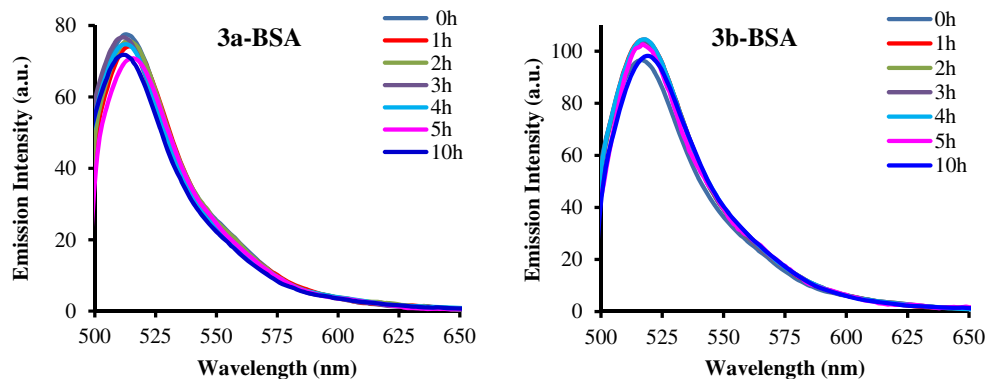
**Fig. 7** **a** Fluorescence spectra of BSA-3b conjugate (*left*) and normalised spectra (*right*). **b** Fluorescence spectra of Egg Albumin-3b conjugate (*left*) and normalised spectra (*right*). **c** Fluorescence spectra of Gelatin-3b conjugate (*left*) and normalised spectra (*right*)



compounds increases with increasing pH of the solution. The fluorescence intensity is less at pH 5 and gradually increases as pH of the solution increases from 5 to 7. A sudden increase in fluorescence intensity was observed for the compounds at pH

of solution 8 and was almost constant for pH 9–12. The emission spectra of the compounds at various pH are shown in Fig. 2. The red shift in emission was observed for pH 8–12 in comparison to pH 5–7. The normalized emission spectra of



**Fig. 8** Stability study of 3a-BSA and 3b-BSA conjugates

compound 3a and 3b is shown in Fig. 3. In both the compounds a red shift around 5 nm was observed for basic pH.

It is well known that fluorescence properties of fluorescein derivatives depend on microenvironment. To study the effect of viscosity on fluorescence emission, mixtures of glycerin: water was used [45]. As the amount of glycerin in solution increases, the fluorescence intensity of the compounds 3a and 3b decreases, while the fluorescence emission maxima remains same for both compounds at different viscosity. The results of fluorescence emission with respect to percentage of glycerol are shown in Fig. 4 and normalized emission spectra are shown in Fig. 5.

### Bioconjugation Study

The conjugation of fluorophores 3a and 3b were carried out with different proteins. The conjugates were analysed by fluorescence spectroscopy. The fluorescence spectra for different hapten-protein conjugates showed gradual decrease in fluorescence intensity with increase in protein-fluorophore molar ratio. The decrease in fluorescence intensity of fluorophores is due to increase in the number of amide bonds formed between the surface lysine groups of the protein and carboxylated fluorophores. This gradual shift in the fluorescence signal or quenching of tryptophan intensity with different conjugates thus confirms the course of hapten-protein conjugation. At low protein-fluorophore concentration, the fluorescence intensity is high; at particular hapten-protein ratio, the intensity became constant. In the case of fluorophore 3a good conjugation results are observed with protein BSA and egg albumin, while fluorophore 3b shows constant conjugation results with studied proteins. In the case of fluorophores 3a–3b, linear trend is observed in fluorescence quenching. The conjugates show slight red shift in emission spectra at higher concentration of fluorophores. The emission spectra and normalised emission spectra of the fluorophore-protein conjugates are shown in Figs. 6 and 7. The stability of fluorophore-protein conjugate is an important parameter for sensing applications. To confirm the stability of conjugates, the stability study of 3a-BSA protein and 3b-BSA protein were performed for period

of 10 h. The results of fluorescence intensity with respect to time are presented in Fig. 8. The stability results of conjugates conclude that, the fluorescence intensity remains same over the period of 10 h.

### Conclusion

In summary, two fluorescein derivatives, which are analogues of FITC dye were synthesized. The compounds show absorption between 490 and 500 nm and emission between 511 and 520 nm ( $\Phi_F \sim 60\%$ ). The experimental photophysical properties are well in line with theoretical data obtained by DFT computation. The % deviation between experimental absorption and vertical excitation is 12 % and the % deviation between TD-DFT emission and experimental emission is 3 %. The significant enhancement of fluorescence intensity of compounds was observed at pH 8. Similar to pH, the fluorescence intensity of 3a and 3b are sensitive towards viscosity of the medium, the fluorescence intensity is medium is more viscous. The compounds 3a and 3b have good binding affinity with BSA, egg albumin and gelatin proteins. The fluorescence intensity of conjugates decreases as the amount of fluorophores increases.

**Acknowledgments** Rahul Telore is thankful to UGC-CAS for research fellowship under Special Assistance Programme (SAP). Santosh Chemate (JRF/SRF) and Dr. Vikas Padalkar (Post-doctoral research fellow) are thankful for fellowship from the Principal Scientific Adviser (PSA), Government of India.

### References

- Vendrell M, Zhai D, Er JC, Chang YT (2012) Combinatorial strategies in fluorescent probe development. *Chem Rev* 112:4391–4420. doi:10.1021/cr200355j
- Sameiro M, Gonçalves T (2009) Fluorescent labeling of biomolecules with organic probes. *Chem Rev* 109:190–212. doi:10.1021/cr0783840

3. Carter KP, Young AM, Palmer AE (2014) Fluorescent sensors for measuring metal ions in living systems. *Chem Rev* 114:4564–4601. doi:10.1021/cr400546e
4. Han J, Burgess K (2010) Fluorescent indicators for intracellular pH. *Chem Rev* 110:2709–2728. doi:10.1021/cr900249z
5. Zhang X, Yin J, Yoon J (2014) Recent advances in development of chiral fluorescent and colorimetric sensors. *Chem Rev* 114:4918–4959. doi:10.1021/cr400568b
6. Sinkeldam RW, Greco NJ, Tor Y (2010) Fluorescent analogs of biomolecular building blocks: design, properties, and applications. *Chem Rev* 110:2579–2619. doi:10.1021/cr900301e
7. Chen X, Pradhan T, Wang F et al (2012) Fluorescent chemosensors based on spiro-ring-opening of xanthenes and related derivatives. *Chem Rev* 112:1910–1956. doi:10.1021/cr200201z
8. Haugland RP (2002) Haugland R (2002) Handbook of fluorescent probes and research products. Molecular Probes, Pennsylvania State University
9. Ambrose WP, Goodwin PM, Jett JH et al (1999) Single molecule fluorescence spectroscopy at ambient temperature. *Chem Rev* 99:2929–2956. doi:10.1021/cr980132z
10. Li C, Liu M, Pschirer NG et al (2010) Polyphenylene-based materials for organic photovoltaics. *Chem Rev* (Washington, DC, United States) 110:6817–6855. doi:10.1021/cr100052z
11. Loudet A, Burgess K (2007) BODIPY dyes and their derivatives: syntheses and spectroscopic properties. *Chem Rev* 107:4891–4932. doi:10.1021/cr078381n
12. Li X, Gao X, Shi W, Ma H (2014) Design strategies for water-soluble small molecular chromogenic and fluorogenic probes. *Chem Rev* 114:590–659. doi:10.1021/cr300508p
13. Cohen B, Martin C, Iyer SK et al (2012) Single dye molecule behavior in fluorescent core-shell silica nanoparticles. *Chem Mater* 24:361–372. doi:10.1021/cm203196w
14. Bhagi A, Pandey S, Pandey A, Pandey S (2013) Fluorescein prototropism within poly(ethylene glycol)s and their aqueous mixtures. *J Phys Chem B* 117:5230–5240. doi:10.1021/jp402113s
15. Chen X, Pradhan T, Wang F et al (2012) Fluorescent chemosensors based on spiro-ring-opening of xanthenes and related derivatives. *Chem Rev* 112:1910–1956. doi:10.1021/cr200201z
16. Andrew TL, Swager TM (2007) A fluorescence turn-on mechanism to detect high explosives RDX and PETN. *J Am Chem Soc* 129:7254–7255. doi:10.1021/ja071911c
17. Chen X, Li Z, Xiang Y, Tong A (2008) Salicylaldehyde fluorescein hydrazone: a colorimetric logic chemosensor for pH and Cu(II). *Tetrahedron Lett* 49:4697–4700. doi:10.1016/j.tetlet.2008.05.137
18. Zou W-S, Zou F-H, Shao Q et al (2014) A selective fluorescent resonance energy transfer quenching and resonance light scattering enhancement dual-recognition probe for 2,4,6-trinitrotoluene. *J Photochem Photobiol A Chem* 278:82–88. doi:10.1016/j.jphotochem.2014.01.002
19. Salleres S, López Arbeloa F, Martínez V et al (2009) Photophysics of rhodamine 6G laser dye in ordered surfactant (C12TMA)/Clay (Laponite) hybrid films. *J Phys Chem C* 113:965–970. doi:10.1021/jp806553p
20. Hilgendorff M, Sundström V (1998) Ultrafast electron injection and recombination dynamics of dye sensitized TiO<sub>2</sub> particles. *Chem Phys Lett* 287:709–713. doi:10.1016/S0009-2614(98)00242-5
21. Moser J, Graetzel M (1984) Photosensitized electron injection in colloidal semiconductors. *J Am Chem Soc* 106:6557–6564. doi:10.1021/ja00334a017
22. Dhami S, de Mello AJ, Rumbles G et al (1995) Phthalocyanine fluorescence at high concentration: dimers or reabsorption effect? *Photochem Photobiol* 61:341–346. doi:10.1111/j.1751-1097.1995.tb08619.x
23. Sednev MV, Wurm CA, Belov VN, Hell SW (2013) Carborhodol: a new hybrid fluorophore obtained by combination of fluorescein and carbopyronine dye cores. *Bioconjug Chem* 24:690–700. doi:10.1021/bc300673z
24. Goldsmith CR, Jaworski J, Sheng M, Lippard SJ (2006) Selective labeling of extracellular proteins containing polyhistidine sequences by a fluorescein-nitrotriacetic acid conjugate. *J Am Chem Soc* 128:418–419. doi:10.1021/ja0559754
25. Chevalier A, Dubois M, Le Joncour V et al (2013) Synthesis, biological evaluation, and in vivo imaging of the first camptothecin-fluorescein conjugate. *Bioconjug Chem*. doi:10.1021/bc3005304
26. Abebe FA, Eribal CS, Ramakrishna G, Sinn E (2011) A “turn-on” fluorescent sensor for the selective detection of cobalt and nickel ions in aqueous media. *Tetrahedron Lett* 52:5554–5558. doi:10.1016/j.tetlet.2011.08.072
27. Li N, Tang W, Xiang Y et al (2010) Fluorescent salicylaldehyde hydrazone as selective chemosensor for Zn<sup>2+</sup> in aqueous ethanol: a ratiometric approach. *Luminescence* 25:445–451. doi:10.1002/bio.1175
28. Zhao Z-G, Shen T, Xu H-J (1989) The absorption and structure of fluorescein and its ethyl derivatives in various solutions. *Spectrochim Acta Part A Mol Spectrosc* 45:1113–1116. doi:10.1016/0584-8539(89)80189-8
29. Crosby GA, Demas JN (1971) Measurement of photoluminescence quantum yields. *Review. J Phys Chem* 75:991–1024. doi:10.1021/j100678a001
30. Kruszewski S, Wybranowski T, Cyrankiewicz M et al (2008) Enhancement of FITC fluorescence by silver colloids and silver island films. *Acta Phys Pol A* 113:1599–1608
31. Williams ATR, Winfield SA, Miller JN (1983) Relative fluorescence quantum yields using a computer-controlled luminescence spectrometer. *Analyst* 108:1067. doi:10.1039/an9830801067
32. Magde D, Wong R, Seybold PG (2002) Fluorescence quantum yields and their relation to lifetimes of rhodamine 6G and fluorescein in nine solvents: improved absolute standards for quantum yields. *Photochem Photobiol* 75:327–334. doi:10.1562/0031-8655(2002)0750327FQYATR2.0.CO2
33. Nakajima N, Ikada Y (1995) Mechanism of amide formation by carbodiimide for bioconjugation in aqueous media. *Bioconjug Chem* 6:123–130. doi:10.1021/bc00031a015
34. Treutler O, Ahlrichs R (1995) Efficient molecular numerical integration schemes. *J Chem Phys* 102:346. doi:10.1063/1.469408
35. Becke AD (1993) A new mixing of Hartree–Fock and local density-functional theories. *J Chem Phys* 98:1372. doi:10.1063/1.464304
36. Lee C, Yang W, Parr RG (1988) Development of the Colle-Salvetti correlation-energy formula into a functional of the electron density. *Phys Rev B* 37:785–789. doi:10.1103/PhysRevB.37.785
37. Luber S, Adamczyk K, Nibbering ETJ, Batista VS (2013) Photoinduced proton coupled electron transfer in 2-(2'-hydroxyphenyl)-benzothiazole. *J Phys Chem A* 117:5269–5279. doi:10.1021/jp403342w
38. Santra M, Moon H, Park M-H et al (2012) Dramatic substituent effects on the photoluminescence of boron complexes of 2-(benzothiazol-2-yl)phenols. *Chemistry* 18:9886–9893. doi:10.1002/chem.201200726
39. Li H, Niu L, Xu X et al (2011) A comprehensive theoretical investigation of intramolecular proton transfer in the excited states for some newly-designed diphenylethylene derivatives bearing 2-(2-hydroxy-phenyl)-benzotriazole part. *J Fluoresc* 21:1721–1728. doi:10.1007/s10895-011-0867-6
40. Wiley: AB INITIO molecular orbital theory - Warren J. Hehre, Leo Radom, P. von R. Schleyer, et al. <http://as.wiley.com/WileyCDA/WileyTitle/productCd-0471812412.html>. Accessed 23 Mar 2015
41. Lakowicz JR (2007) Principles of fluorescence spectroscopy (Google eBook). 980
42. Patil VS, Padalkar VS, Tathe AB, Sekar N (2013) ESIPT-inspired benzothiazole fluorescein: photophysics of microenvironment pH

- and viscosity. *Dye Pigment* 98:507–517. doi:[10.1016/j.dyepig.2013.03.019](https://doi.org/10.1016/j.dyepig.2013.03.019)
43. Bauernschmitt R, Ahlrichs R (1996) Treatment of electronic excitations within the adiabatic approximation of time dependent density functional theory. *Chem Phys Lett* 256:454–464. doi:[10.1016/0009-2614\(96\)00440-X](https://doi.org/10.1016/0009-2614(96)00440-X)
44. Kwon JE, Park SY (2011) Advanced organic optoelectronic materials: harnessing excited-state intramolecular proton transfer (ESIPT) process. *Adv Mater* 23:3615–3642. doi:[10.1002/adma.201102046](https://doi.org/10.1002/adma.201102046)
45. Sheely ML, Works AS, Ill C (1932) Glycerol viscosity tables. *Ind Eng Chem* 24(9):1060–1064